Int. J. of Applied Mechanics and Engineering, 2005, vol. 10, No. 3, pp. 451-462

POISSON RATIO EFFECTS AND CRITICAL VALUS IN SPHERICAL AND CYLINDRICAL HERTZIAN CONTACTS

Itzhak Green
Georgia Institute of Technology
G. W. Woodruff School of Mechanical Engineering
Atlanta, GA 30332-0405, USA
e-mail: itzhak.green@me.gatech.edu

1. ABSTRACT

This work determines the location of the greatest elastic distress in spherical and cylindrical Hertzian contacts based upon the distortion energy and the maximum shear stress theories. The ratios between the maximum pressure, the von Mises stress, and the maximum shear stress are determined and fitted by empirical formulations for a wide range of the Poisson ratio, which represents material compressibility. Some similarities exist between cylindrical and spherical contacts, where for many metallic materials the maximum von Mises or shear stresses emerge beneath the surface. However, in cylindrical contact if any of the materials is excessively compressible then the maximum von Mises stress appears at the surface. The corresponding Poisson ratios are found. The critical forces that cause yielding onset, and the corresponding interferences and radius or half-width contact are derived along with the maximum stored strain energy. It is shown that the distressing stresses decrease as Poisson's ratio increases (i.e., as the material approaches incompressibility). The results obtained herein are then used to calibrate FEA meshes intended for cases that do not have closed-form solutions.

2. INTRODUCTION

The utility of the Hertzian [1] solution in engineering is vast, and likewise the literature is rich with theory and applications. In mechanical engineering applications (gears, bearings, rail-and-wheel, etc.) it is common to find solutions that are specific to a single Poisson ratio that equals to 0.3, serving as a "representative" value for metallic materials. This work uses the Hertzian solution for spherical and cylindrical contact for a wide range of Poisson ratios, $0 \le \nu \le 1/2$. Some of the results are as expected (e.g., maximum distress beneath the surface under certain conditions), but some of the results have not been encountered or derived before. The results are both useful to calculate critical values for design, and valuable for the calibration and convergence of FEA codes for both types of contact.

Spherical contact has received considerable attention in the last four decades particularly because of its applicability to asperity contact. A spherical contact is shown in Fig. 1a, for which the maximum elastic deflection based upon the Hertz solution is (Johnson [2])

$$\omega = \left(\frac{\pi p_o}{2E'} \right)^2 R \; ; \quad \frac{1}{E'} = \frac{1-\nu_1^2}{E_1} + \frac{1-\nu_2^2}{E_2} \; ; \; \frac{1}{R} = \frac{1}{R_1} + \frac{1}{R_2} \tag{1}$$

where p_o is the maximum Hertzian pressure, and E_1, ν_1, R_1, E_2, ν_2, R_2, are the elastic properties and radii of sphere 1 and 2, respectively. It is well known that for spherical contact the maximum von Mises stress occurs under the surface, and thus yielding onset would take place at that location. Using the "meaning" of hardness (Tabor [3]) a critical interference and plasticity index are derived by Greenwood and Williamson [4]. That critical interference is given by

$$\omega_c = 0.89R\left(\frac{H}{E'}\right)^2 \tag{2}$$

where an assumption in [4] is made that p_o is about $0.6H$, and H is the material hardness. Chang et al. [5] have similarly presented a critical interference

$$\omega_c = \left(\frac{\pi KH}{2E'}\right)^2 R \tag{3}$$

This critical interference is identical to that given in Eq. (2) if one lets the hardness factor $K=0.6$. To accommodate various Poisson ratios, a linear expression is proposed, $K = 0.454 + 0.41\nu$, which again is derived based upon the definition of hardness, using a fixed relationship $H=2.8S_y$, where S_y is the material yield strength.

The conceptual drawback imbedded in Eqs. (2, 3) is that they rely upon "hardness," a loosely defined quantity (see Williams [6]) that, if one adopts a common definition that has gained status in the field, equals to the average indentation pressure that occurs during fully plastic flow of the entire contact area. This state is vastly distinct from what ω_c represents; i.e., ω_c is the interference that causes yielding onset at a single point beneath the surface, and it is derived from pure elastic considerations. Hardness on the other hand deals with "full plasticity" of the entire contact surface and, therefore, it can hardly be relevant to this case. A hardness geometric limit has been defined and discussed by Jackson and Green [7], which is shown to vary not only with material properties but also with the contact geometry of the surface; i.e., with the deformation itself. That is, the factor of 2.8 in $H=2.8S_y$ may only be considered as a first approximation, where other factors may need to be used instead. Of course, if hardness is defined solely based upon yield strength then it is redundant, and clearly is not an independent material property.

Avoiding the (unnecessary) definition of hardness, an alternate derivation is proposed which uses the distortion energy yield criterion at the site of maximum von Mises stress. To determine yielding the von Mises stress is directly compared against the well-defined yield strength property, S_y. The alternate derivation is proposed in [7] but is limited to determining critical interference for spherical contact only. It will be expanded to determine other critical parameters as well. These are not only of value from a practical design viewpoint but are also of greatest importance for FEA modeling of Hertzian contacts. Such FEA contact models are difficult to converge, and the limits of elastic behavior, if known a priori, would be of value to establish mesh convergence. In most commercial FEA codes the yield strength is a common material input, where hardness is not.

The modeling of various machine elements such as gears, rolling element bearings, or wheel-on-rail, lends itself to elliptical contact and in the limit (say for needle bearings) takes on a cylindrical form of contact. Critical parameters are sought in this work also for a cylindrical contact, which include the critical force that causes yielding onset, and the corresponding interferences and half-width contact. It is found that maximum distress may occur at the surface or beneath it depending on Poisson's ratio. Hence, far away from the contact ends where the state of plane strain prevails, the stresses are considerably lower than at the ends where the state of plane stress prevails.

3. SPHERICAL HERTZIAN STRESS

Let the x and y axes reside in the circular area of contact between the two spheres, and the z axis is the coordinate into the spheres (see Fig. 1a). The maximum (and principal) stresses occur at $x=y=0$. Under the total load, P, the maximum pressure is generated at the origin (Johnson [2])

$$p_o = \frac{3P}{2\pi a^2} = \frac{1}{\pi}\left[6P\left(\frac{E'}{R}\right)^2\right]^{1/3} \tag{4}$$

where the Hertzian contact radius is given by:

$$a = \left(\frac{3PR}{4E'} \right)^{1/3} \tag{5}$$

and the deflection is given by Eq. (1). Defining $\zeta = | z / a |$, then the stresses for the spherical contact, as given by Shigley [8], are

$$\sigma_x = \sigma_y = \left\{ \frac{1}{2(1+\zeta^2)} - (1+\nu) \left(1 - \zeta \, \text{ArcTan}\left[\frac{1}{\zeta} \right] \right) \right\} p_o \tag{6}$$

$$\sigma_z = -\frac{p_o}{1+\zeta^2} \tag{7}$$

These stresses are calculated in either material 1 or 2, permitting obviously only $\zeta \geq 0$ in both materials. While σ_z is independent of Poisson's ratio, σ_x and σ_y are both dependent upon it. While the theoretical limit of Poisson's ratio is between $-1 < \nu \leq 1/2$, it is rare to encounter engineering materials with negative Poisson ratios. Most materials will fall in the range $0 \leq \nu \leq 1/2$ and the discussion herein is limited to this range.

3.1 MAXIMUM VON MISES STRESS AND CRITICAL PARAMETERS

Based upon Eqs. (6, 7) the von Mises stress, σ_e, normalized by the contact pressure, p_o, is calculated by:

$$\frac{\sigma_e}{p_o} = \frac{1}{2} \sqrt{\frac{(1 - 2\nu - 2\zeta^2 (1+\nu) + 2(\zeta + \zeta^3)(1+\nu) \, \text{ArcCot}[\zeta])^2}{(1+\zeta^2)^2}} \tag{8}$$

The above varies with ζ where ν is a parameter. A plot of this ratio is given in Fig. 2. Notably there is a single stationary point that resides inside the material signifying the point of greatest distress. The maximum von Mises stress is obtained by letting $d(\sigma_e / p_o)/d\zeta = 0$. Applying that to Eq. (8) and considering just the numerator gives,

$$\left(-\zeta (4 + \nu + \zeta^2 (1+\nu)) + (1+\zeta^2)^2 (1+\nu) \, \text{ArcCot}[\zeta] \right) (1 - 2\nu - 2\zeta^2 (1+\nu) + 2(\zeta + \zeta^3)(1+\nu) \, \text{ArcCot}[\zeta]) = 0 \tag{9}$$

This transcendental equation is solved numerically for ζ_m where ν as a parameter is varied in the aforementioned range. The solution is curve fitted, giving the location of maximum von Mises stress at

$$\zeta_m = 0.38167 + 0.33136\nu \tag{10}$$

The numerical values of ζ_m (not the curve fitted ones) are substituted back into Eq. (8) for finding the maximum value of σ_e / p_o. Defining its reciprocal, $C = p_o / \sigma_{e-\max}$, results clearly in $C = C(\nu)$. A curve fit procedure gives

$$C = 1.30075 + 0.87825\nu + 0.54373\nu^2 \tag{11}$$

with almost indistinguishable error, where ν is the Poisson ratio of either material (i.e., it is either ν_1, or ν_2). The true interpretation of C is that it represents the ratio between the maximum contact pressure and the maximum von Mises stress. At yielding p_o takes on the critical value p_{oc}, and by definition $\sigma_{e-\max} = S_y$, which gives $C = p_{oc} / S_y$. The maximum von Mises stress occurs beneath the surface at some location, z, which varies with p_o. However, the value of C is determined for the ratio of z/a (a being the contact radius) and thus is independent of z by itself. The same is true for the locus of maximum von Mises stress, i.e., $\zeta_c = \zeta_m$. To obtain the critical interference the value of p_o is replaced with CS_y in Eq. (1), and solving Eq. (4, 5) gives

$$\omega_c = \left(\frac{\pi C S_y}{2E'} \right)^2 R \quad ; \quad P_c = \frac{\left(\pi C S_y\right)^3 R^2}{6E'^2} \quad ; \quad a_c = \frac{\pi C S_y R}{2E'} \tag{12}$$

where $CS_y = \min\left(C(\nu_1)S_{y1}, C(\nu_2)S_{y2}\right)$, accounting for the possibility of two different material properties. The above parameters are useful for design purposes as well as for the calibration and convergence of FEA codes (to be discussed below). Another useful parameter is the potential (strain) energy stored during elastic deformation, equaling to the work done

$$U = \int P d\omega = \frac{8}{15} E' R^{1/2} \omega^{5/2}$$
$$= \int P \frac{d\omega}{dP} dP = \frac{1}{5} \left(\frac{9P^5}{2E'^2 R} \right)^{(1/3)}$$

The result is expressed by either the deflection (interference), or load. Substituting Eq. (12) in the above results in the maximum elastic energy that can possibly be stored (i.e., on the verge of yielding, or plastic deformation)

$$U_c = \frac{\left(\pi C S_y\right)^5 R^3}{60E'^4} \tag{13}$$

In the above it is idealized that linear elasticity prevails to yielding. While the strain energy is given for the entire conjunction that includes both elastic bodies, it is apportioned amongst them based upon their relative stiffness.

3.2 MAXIMUM SHEAR STRESS AND CRITICAL PARAMETERS

Oftentimes the maximum shear stress is used to determine distress. Defined as $\tau_{\max} = \max\left(|\sigma_x - \sigma_y|, |\sigma_y - \sigma_z|, |\sigma_z - \sigma_x|\right)/2$, then substitution of Eqs. (6, 7) results in

$$\tau_{max}/p_o = \frac{1}{2}\left(-1 + \frac{3}{2(1+\zeta^2)} - \nu + \zeta(1+\nu)\,\mathrm{ArcCot}[\zeta]\right) \tag{14}$$

where the *max()* function in this hemispherical contact simplifies into a single expression because the x and y stresses are identical. The plot of this stress as a function of depth and for various Poisson ratios is given in Fig. 3. Sometimes stress intensity is used instead, $\sigma_I = \max\left(|\sigma_x - \sigma_y|, |\sigma_y - \sigma_z|, |\sigma_z - \sigma_x|\right)$. Hence, doubling the values of the ordinate in Fig. 3 gives the latter.

3.3 DISCUSSION OF RESULTS

The von Mises stress and maximum shear stress behave very similarly. In fact, the maximum shear stress analysis does not add new information (however, for some materials the application of the latter theory may be more suitable for failure). Both normalized stresses have stationary points (and thus distress points) beneath the surface, where the maximum stresses are getting larger with increasing material compressibility (i.e., lower Poisson ratio). This can be explained by the hydrostatic (or average) stress component that increases with the tendency of incompressibility (i.e., larger Poisson ratio). Since this hydrostatic component is ultimately being eliminated from the final outcome of the von Mises and shear stresses, it results in lower ultimate values. Hence, from a design perspective, tendency to larger Poisson ratios is desirable.

4. CYLINDRICAL HERTZIAN STRESS

While some of the general trends from spherical contact pertain to cylindrical contact, the behavior of the latter is more complex as shall be seen. Let *x* be the axis along the line of contact, the *y* axis is tangent to the two cylinders, and the *z* axis is the coordinate into the cylinders (see Fig. 1b). The maximum (and principal) stresses occur at *x=y=0*. Under a total load per unit length, *P/L*, maximum pressure is generated at the origin (Johnson [2])

$$p_o = \frac{2P}{\pi bL} \tag{15}$$

where the Hertzian half-width is given by:

$$b = \left(\frac{4(\lambda_1 + \lambda_2)PR_1R_2}{L(R_1 + R_2)} \right)^{1/2} = \left(\frac{4PR}{\pi LE'} \right)^{1/2};\ \lambda_i = \frac{1-\nu_i^2}{\pi E_i};\quad i = 1,2 \tag{16}$$

Now redefining $\zeta = | z / b |$, then the stresses for cylindrical contact are (Shigley [8])

$$\sigma_y = -\left(-2\zeta + \sqrt{1+\zeta^2}\left(2 - \frac{1}{1+\zeta^2} \right) \right) p_o \tag{17}$$

$$\sigma_z = -\frac{p_o}{\sqrt{1+\zeta^2}} \tag{18}$$

These two stresses are calculated in either material 1 or 2, where again only $\zeta \geq 0$ is allowed in both materials, noting that both are independent of Poisson's ratio. Assuming the state of plain strain then the transverse stress is $\sigma_x = \nu(\sigma_z + \sigma_y)$ which reduces to,

$$\sigma_x = -2\left(-\zeta + \sqrt{1+\zeta^2} \right) \nu\, p_o \tag{19}$$

As previously, the discussion is limited to the range $0 \leq \nu \leq 1/2$. Conveniently, letting ν approach zero leads to a bi-axial stress state (i.e., plane stress).

4.1 MAXIMUM VON MISES STRESS AND CRITICAL PARAMETERS

Based upon Eqs. (17-19) the von Mises stress, σ_e, normalized by the contact pressure, p_o, is calculated by:

$$\frac{\sigma_e}{p_o} = \sqrt{-\frac{\left(-1+2\zeta\left(-\zeta+\sqrt{1+\zeta^2}\right)\right)\left(1+4\zeta^2+4\left(1+\zeta^2\right)\left(-1+\nu\right)\nu\right)}{1+\zeta^2}} \tag{20}$$

The above varies with ζ, where ν is a parameter. A plot of this ratio is given in Fig. 4. It is noted that the maximum von Mises stress can occur either on the surface (*z/b=0*) or somewhere under the surface (*z/b>0*) depending upon Poisson's ratio. The threshold is found below, but the fact that the maximum von Mises stress may be positioned at the surface is unique to cylindrical contact (as opposed to spherical contacts where the maximum von Mises stress is always under the surface for all said Poisson ratios). The reason why this happens in the case of cylindrical contact is imbedded in the assumption of plane strain where σ_x is linearly dependent upon the Poisson ratio (see Eq. (19)). As ν diminishes the tri-axial stress state tends to a bi-axial stress state, leading to a higher von Mises stress for the same load, *P* or p_o. At $\zeta = 0$ Eq. (20) degenerates to

$$\left[\frac{\sigma_e}{p_o}\right]_{\zeta=0} = \sqrt{1+4(\nu-1)\nu} \tag{21}$$

For perfect compressibility, $\nu = 0$, and at $\zeta = 0$ a theoretical value is obtained, $\sigma_e / p_o = 1$.

The maximum von Mises stress is obtained by letting $d(\sigma_e / p_o)/d\zeta = 0$; hence, applying to Eq. (20) and considering the numerator only gives,

$$\begin{aligned}&-1+\zeta\left(5\sqrt{1+\zeta^2}+\zeta\left(-13+4\zeta\left(4\sqrt{1+\zeta^2}+\zeta\left(-5+2\zeta\left(-\zeta+\sqrt{1+\zeta^2}\right)\right)\right)\right)\right)-\\&4\left(1+\zeta^2\right)^2\left(-1+2\zeta\left(-\zeta+\sqrt{1+\zeta^2}\right)\right)\nu+4\left(1+\zeta^2\right)^2\left(-1+2\zeta\left(-\zeta+\sqrt{1+\zeta^2}\right)\right)\nu^2=0\end{aligned} \tag{22}$$

This equation is solved numerically for ζ_m where ν as a parameter is varied in the aforementioned range. The value of ζ_m is substituted back into Eq. (20) for finding the maximum value of $\sigma_e / p_o \triangleq C^{-1}$, where again $C = C(\nu)$. As discussed above, a global maximum stationary point exists only above a certain value of ν. Up to that value the maximum is at the surface according to Eq. (21). An exhaustive search reveals that at $\nu = 0.1938$, the transition occurs at a value of $C^{-1} = \sigma_e / p_o = 0.6122$ with an error of 10^{-4}. The behavior of σ_e / p_o for this specific value of $\nu = 0.1938$ is also shown in Fig. 4. Beyond $\nu = 0.1938$ the numerical values of $C(\nu)$ are curve fitted to a parabolic expression given below in Eq. (23), with almost indistinguishable error,

$$C = \begin{cases} \dfrac{1}{\sqrt{1+4(\nu-1)\nu}} & ;\ \zeta_m = 0 \qquad @ \quad \nu \le 0.1938 \\ 1.164+2.975\nu-2.906\nu^2 & ;\ \zeta_m = 0.223+2.321\nu-2.397\nu^2 \qquad @ \quad \nu > 0.1938 \end{cases} \tag{23}$$

This value of *C* is valid for as long as the material is elastic, i.e., up to yielding onset. This value is used to calculate critical parameters. The maximum deformation in a cylindrical line contact is given by Hamrock [9]. In the current notation it is

$$\delta = \frac{1}{\pi E'}\frac{P}{L}\left[\ln\left(\frac{4\pi E' R}{P/L}\right)-1\right]$$

If the distortion energy (von Mises) theory is used to predict yielding onset, then with the aid of Eq. (15) and the definition of *C*, the critical values for force per unit length, interference, and half-width are derived,

$$\frac{P_c}{L} = \frac{\pi R (CS_y)^2}{E'} \quad ; \quad \delta_c = R\left(\frac{CS_y}{E'}\right)^2\left[2\ln\left(\frac{2E'}{CS_y}\right)-1\right] \quad ; \quad b_c = \frac{2RCS_y}{E'}. \tag{24}$$

where again $CS_y = \min\left(C(\nu_1)S_{y1}, C(\nu_2)S_{y2}\right)$ accounts for two different material properties. The potential (strain) energy per unit length, stored during elastic deformation is calculated by

$$\frac{U}{L} = \int P\frac{d\delta}{dP}dP = \frac{1}{4\pi E'}\left\{2\ln\left[\frac{4\pi E' R}{(P/L)}\right]-3\right\}\left(\frac{P}{L}\right)^2$$

Substituting the ratio of P_c/L from Eq. (24) in the above results in the maximum elastic energy that can possibly be stored (up to the point of yielding onset)

$$\frac{U_c}{L} = \frac{\pi\left(CS_y\right)^4 R^2}{4E'^3}\left\{4\ln\left[\frac{2E'}{CS_y}\right]-3\right\} \tag{25}$$

4.2 MAXIMUM SHEAR STRESS

Using again $\tau_{\max} = \max\left(|\sigma_x-\sigma_y|, |\sigma_y-\sigma_z|, |\sigma_z-\sigma_x|\right)/2$, then upon substitution of Eqs. (17-19) results in

$$\tau_{max}/p_o = \max\left(\begin{array}{c} \zeta - \zeta\nu + \frac{-1+2\zeta^2(-1+\nu)+2\nu}{2\sqrt{1+\zeta^2}} \\ \zeta\left(-1+\frac{\zeta}{\sqrt{1+\zeta^2}}\right) \\ -\frac{1}{2\sqrt{1+\zeta^2}} + \left(-\zeta+\sqrt{1+\zeta^2}\right)\nu \end{array}\right) \tag{26}$$

Fig. 5 indicates that the maximum shear stress occurs at the surface when $\nu = 0$. But for $\nu > 0$ the maximum value appears beneath the surface having a reduced maximum value as ν increases. The function of $\tau_{\max}$ may contain a discontinuity in slop because of the nature of the *max()* function above, leading to two identical stationary points at $\nu \approx 0.24$. Again, the maximum shear stress depends upon the Poisson ratio, and doubling the values of the ordinate in Fig. 5 gives the value of the stress intensity.

4.3 DISCUSSION OF RESULTS

The stress behavior in cylindrical line contact is quite different than that found in spherical contact. First, maximum distress can occur at the contact surface as well as beneath the surface; all this depends upon the Poisson ratio.

Again, unlike in spherical contact the maxima of the von Mises and shear stresses do not behave quite the same. While both have dual maxima, they occur at two different Poisson ratios (0.1938 and 0.24, respectively).

The plane stress state can be obtained by letting the Poisson ratio approach zero (even if the actual value is different than zero). Clearly, this indicates that at the ends of a cylindrical contact the stress can be considerably higher than at regions sufficiently distant from the ends. This may explain the need for crowning that is commonly used in rolling element bearings to mitigate differences in stresses along the line of contact.

5. FEA CONVERGENCE

Details of FEA modeling can be found in Jackson and Green [7], but instead of solving the contact case of a hemisphere against a rigid flat, the FEA solution here is done for two identical elastic contacting half-cylinders (for brevity the case of two contacting hemispheres is omitted, although the trends are identical). Fig. 6 shows the deformed and undeformed geometries, the mesh, and the von Mises stress in the zoomed area of interest. The overall model contains 83372 nodes, 25750 elements (8-node), and 200 contact elements in the region of interest (this model is of similar refinement as in [7]; however, here because two elastic bodies are modeled in full the size of the entire model is more than doubled). A new meshing scheme is introduced in which a semicircular dense region of elements (visible in Fig. 6) is intended to capture the extremely high stresses in the small region of interest. Likewise, the mesh has a reasonable number (which can be adjusted) of contact elements to capture the contact phenomenon. As in [7], interference is applied, and the reactions are obtained from the code. As experience shows FEA codes are notoriously difficult to converge for Hertzian contacts, particularly at the smallest deformations. This is because of the highly nonlinear nature of the contacting problem that is compounded with a finite resolution between the contact elements, and which further worsens with decreasing interferences. Using the results from Eq. (24) the critical values are calculated for $E_1 = E_2$,=200 GPa, $\nu_1=\nu_2$=0.32, and $R1=R2=1$ *m,* and $S_y=0.9115GPa$. Using the commercial code ANSYS®[1], the results of the simulation are given Table 1, where the last row represents the critical values. The relative differences between the numerical values and those calculated based upon the analysis herein are also given for smaller interferences. It is obvious that very good agreement exists for the critical case. The agreement worsens (but not excessively) with decreasing applied interferences. It should be noted that various mesh schemes have been tried, and while having a similar number of nodes and elements the discrepancies were significant (tens of percents difference at the critical value). This reinforces the fact that mesh convergence is of utmost importance, as the mesh itself can introduce overly stiff structures or non-isotropic behavior. The mesh presented here is believed to have given satisfactory results, and it establishes confidence in analyzing contact problems of various kinds for which closed form solutions do not exist.

6. CONCLUSIONS

This work determines the location of the greatest elastic distress in spherical and cylindrical Hertzian contacts based upon the distortion energy and the maximum shear stress theories. The ratios between the maximum pressure, the von Mises stress, and the maximum shear stress are determined and fitted by empirical formulations for a wide range of the Poisson ratio, which represents material compressibility. Some similarities exist between cylindrical and spherical contacts, where for many metallic materials the maximum von Mises or shear stresses emerge beneath the surface. However, if any of the materials in cylindrical contact is excessively compressible then the maximum von Mises stress appears at the surface. The transitional Poisson ratios are found. The critical forces that cause yielding onset, and the corresponding interferences and radius or half-width contact are derived for both types of contact. Likewise, the stored strain energies for both cases are obtained. The definition of hardness is never used in the determination of critical values. It is shown that in general the distressing stresses decrease as Poisson's ratio increases (i.e., as the material approaches incompressibility). The analytical results presented can serve as targets for convergence and calibration of FEA meshes to be used in cases where closed-form solutions are unavailable.

[1] ANSYS® is a registered trademark of SAS IP

ACKNOWLEDGMENT

This is to acknowledge the meticulous work done on the FEA model by Mr. Raghvendra Vijaywargiya. This research is supported in part through the Department of Defense Multidisciplinary Research Program of the University Research Initiative as Office of Naval Research Grant N00014-04-1-0601, entitled "Friction & Wear under Very High Electromagnetic Stress." Dr. P. Peter Schmidt serves as Program Officer. Information conveyed in this manuscript does not necessarily reflect the position or policy of the Government, and no official endorsement should be inferred.

REFERENCES

1. Hertz, H., 1882, *Über die berührung fester elastische körper*, Journal fuer die Reine und angewandte Mathematik, Vol. 92, pp. 156-171.
2. Johnson, K. L., 1985, Contact Mechanics, Cambridge University Press, Cambridge.
3. Tabor, D., 1951, The Hardness of Materials, Clarendon Press, Oxford.
4. Greenwood, J. A. & Williamson, J. B. P. 1966, "Contact of Nominally Flat Surfaces," Proc. R. Soc. Lond. A, 295, pp. 300-319.
5. Chang, W. R., Etsion, I., and Bogy, D. B., 1987, "An Elastic-Plastic Model for the Contact of Rough Surfaces," ASME J. Tribol., 109, pp.257-263.
6. Williams, J. A., 1994, Engineering Tribology, Oxford University Press, Oxford.
7. Jackson, R. L., Green, I., 2005, "A Finite Element Study of Elasto-plastic Hemispherical Contact Against a Rigid Flat," *ASME Trans., J. of Tribology*, Vol. 127, No. 2, pp. 343-354.
8. Shigley, J. E., Mischke, C. R., 1989, Mechanical Engineering Design, 5th Edition, McGraw-Hill Inc., New York.
9. Hamrock, B.J., "Fundamentals of Machine Elements," McGraw-Hill, 1994.

FIGURES

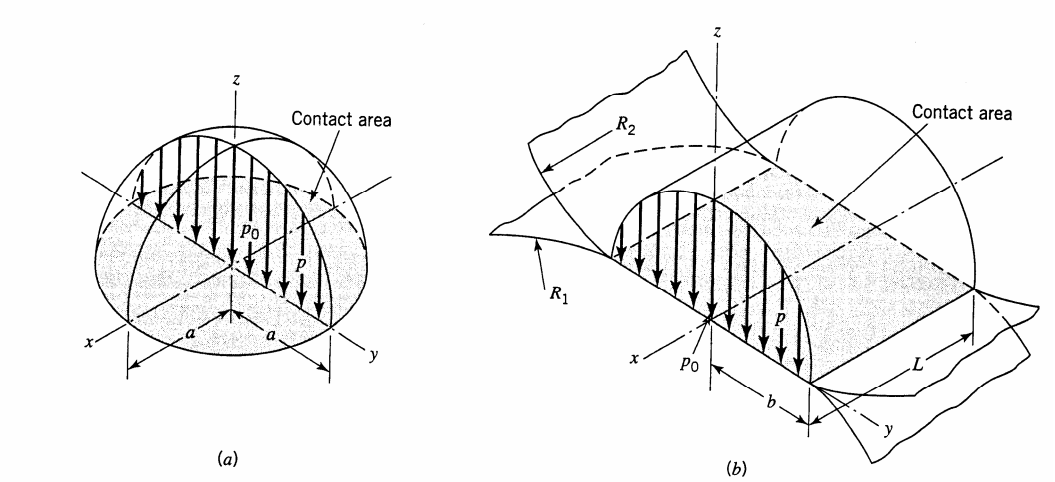

Fig.1: Spherical point contact (a), and cylindrical line contact (b)

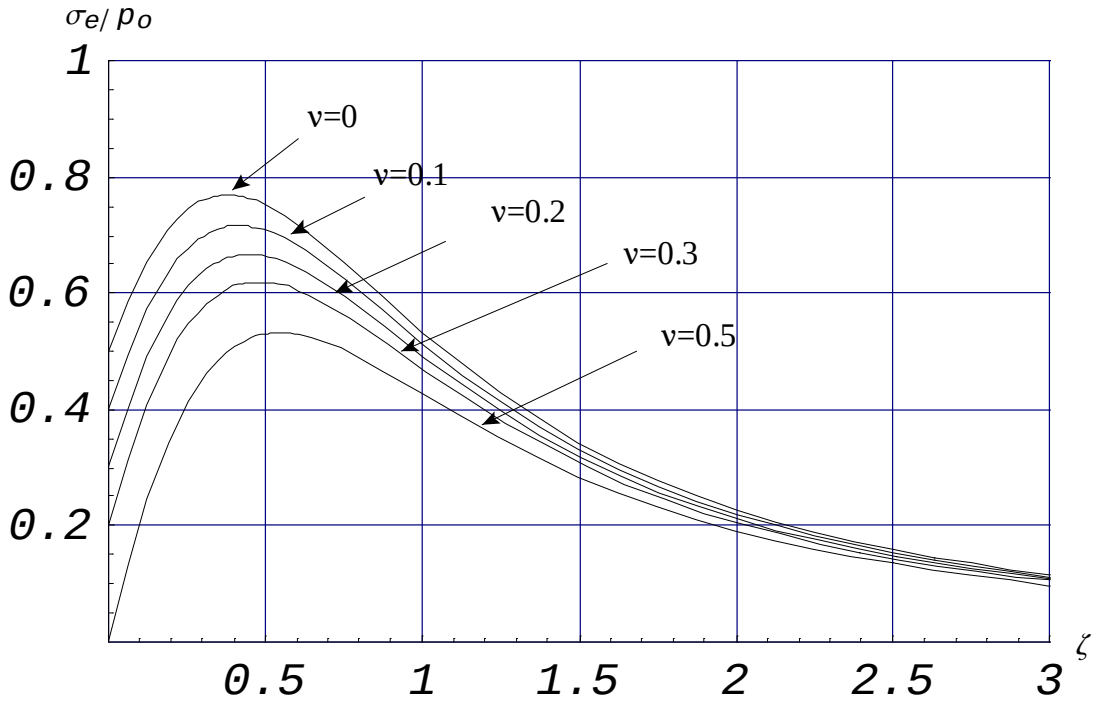

Fig. 2: Normalized von Mises stress for spherical contact as a function of nondimensional |*z/a*| for various Poisson ratios.

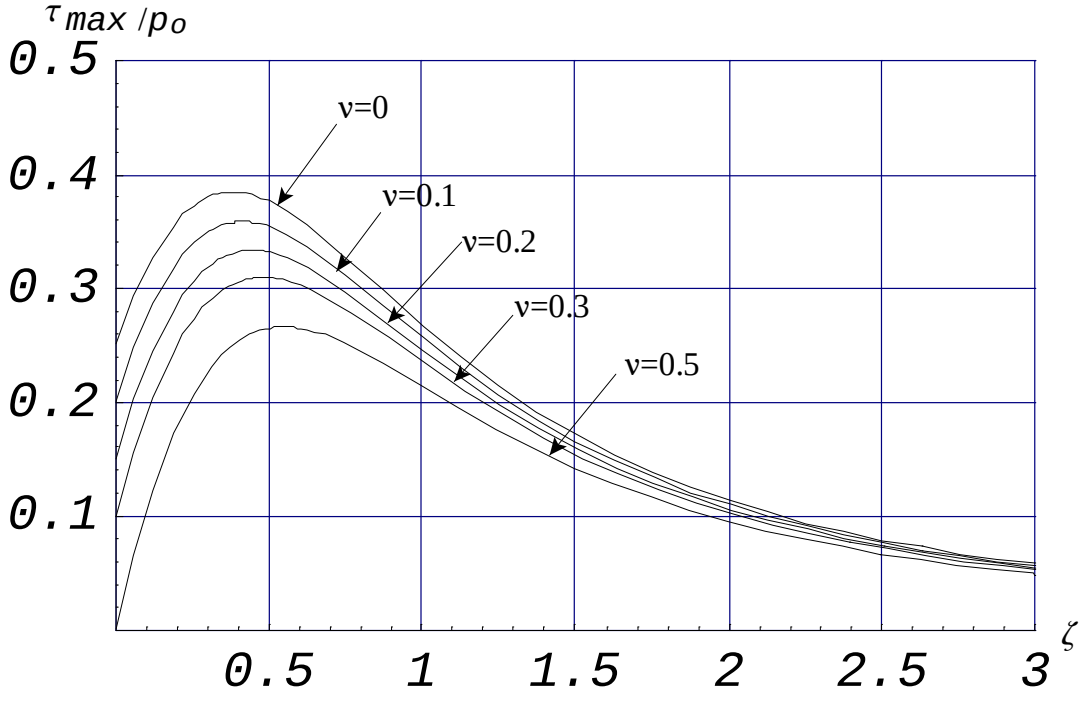

Fig. 3: Normalized maximum shear stress for spherical contact as a function of nondimensional |*z/a*| for various Poisson ratios.

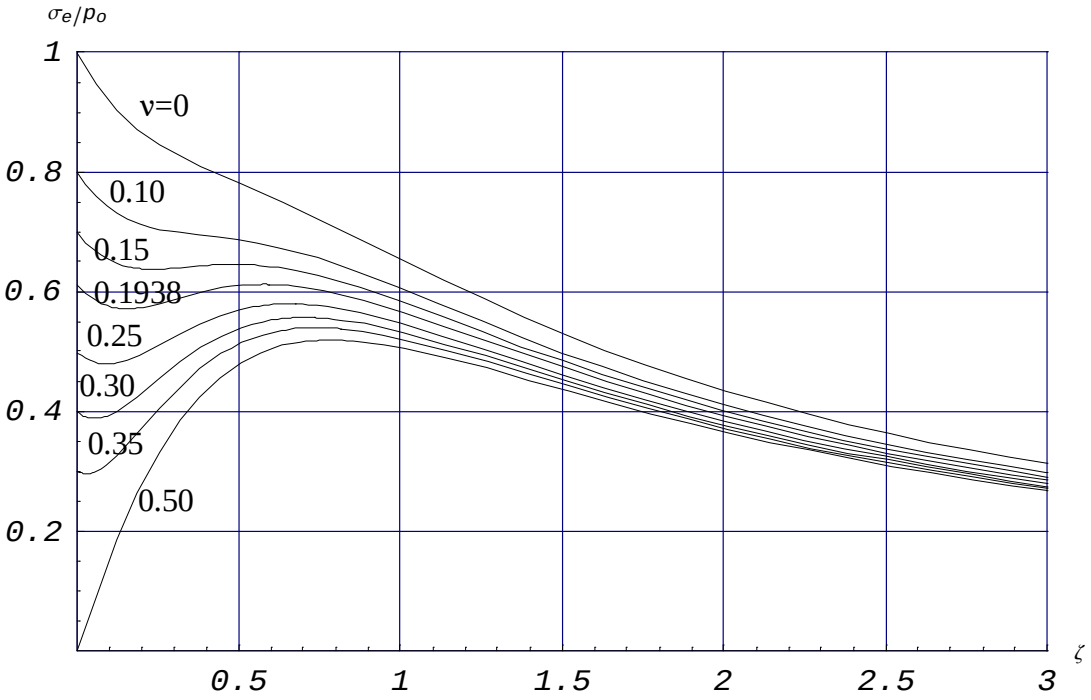

Fig. 4: Normalized von Mises stress for cylindrical contact as a function of nondimensional |*z/b*| for various Poisson ratios.

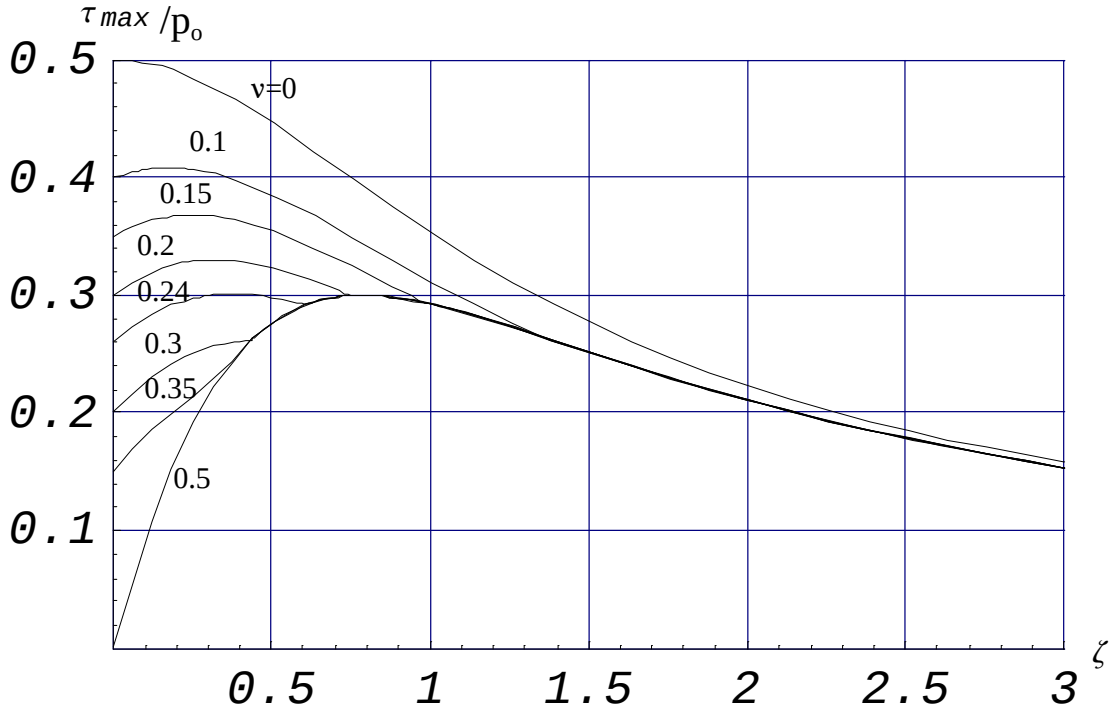

Fig. 5: Normalized maximum shear stress for cylindrical contact as a function of nondimensional |*z/b*| for various Poisson ratios.

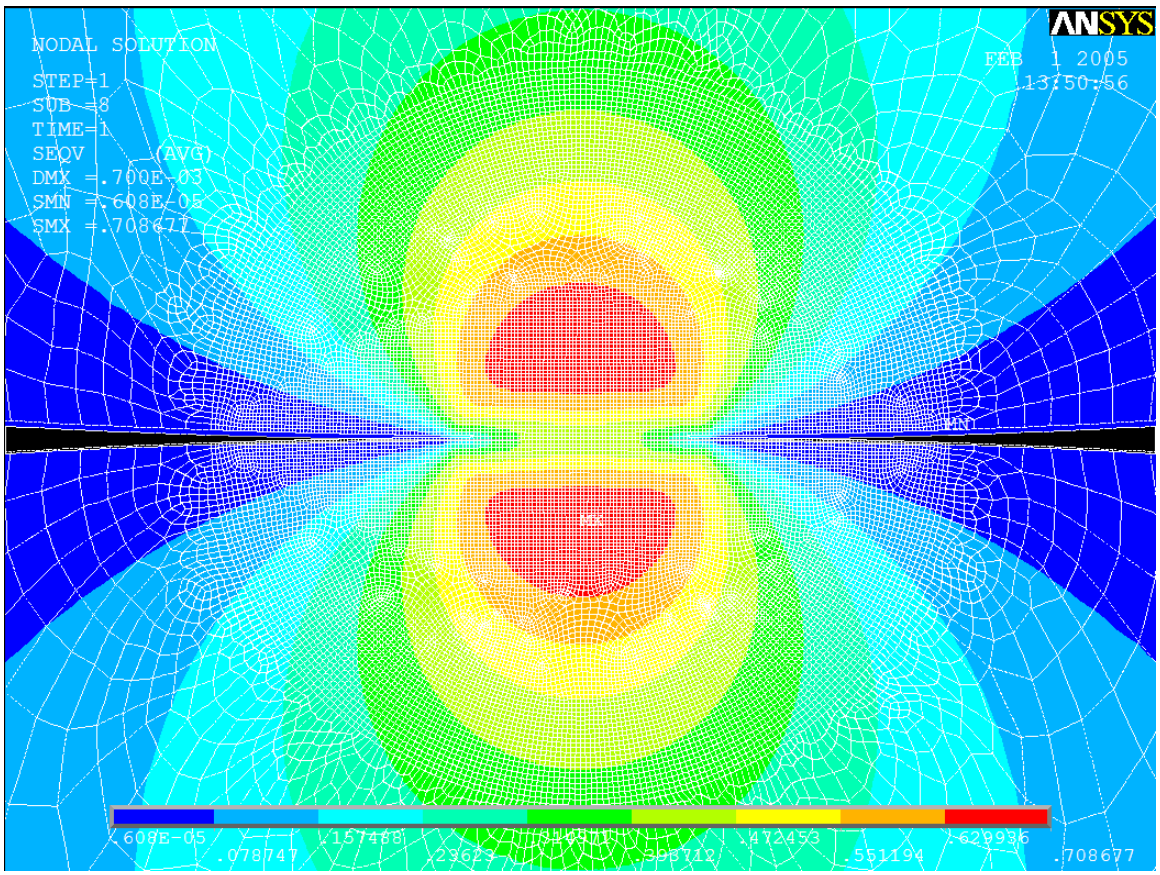

Fig. 6: FEA model (deformed and undeformed geometries) and the von Mises Stress for δ=0.0007 m.

Table 1: Cylinder-on-Cylinder Contact FEM Simulation Results

applied δ [m]	ANSYS b[m]	ANSYS σ_e[GPa]	ANSYS p_o[GPa]	Theoretical b[m]	%diff	Theoretical p_o[GPa]	%diff	Theoretical σ_e[GPa]	%diff
0.0002	0.006625301	0.33803	0.61506	0.005795	-14.33	0.645583	4.728	0.355216	4.838
0.0003	0.007843083	0.43299	0.78559	0.007261	-8.011	0.808976	2.891	0.445119	2.725
0.0005	0.010103994	0.58498	1.0577	0.009642	-4.790	1.074208	1.537	0.591056	1.028
0.0007	0.012016179	0.70868	1.2791	0.011619	-3.417	1.294466	1.187	0.712247	0.501
δ_c=0.00097	0.014446403	0.85777	1.5446	0.013967	-3.431	1.556062	0.737	0.856184	-0.185